Eur. Phys. J. D **1**, 117-128 (1998)

THE EUROPEAN PHYSICAL JOURNAL D

Relativistic distorted-wave calculation of inelastic electron-alkali atom scattering

V. Zeman[a], R.P. McEachran[b], and A.D. Stauffer[c]

Department of Physics and Astronomy, York University, Toronto, Ontario, Canada M3J 1P3

Received: 6 June 1997 / Revised: 3 December 1997 / Accepted: 11 December 1997

Abstract. The relativistic distorted-wave method was used to perform calculations for electron impact excitation of the first $(n\mathrm{p})\,^2\mathrm{P}_{1/2,3/2}$ levels of Na, K and Rb at incident electron energies in the range 20–200 eV. Scattering parameters presented include differential and integrated cross sections, differential and integrated Stokes parameters, generalized STU-parameters and various collisional alignment and orientation parameters. Comparisons with experiment and other theories are in agreement except for cases where first-order methods have been previously proven to be insufficient. Relativistic effects, mainly due to the spin-orbit interaction, have been found to be prominent for rubidium.

PACS. 34.80.Dp Atomic excitation and ionization by electron impact – 34.80.Nz Spin dependence of cross sections; polarized electron beam experiments

1 Introduction

Electron-atom scattering is currently a very rapidly expanding field. This is due in part to recent advances which have greatly increased the quality in the production and detection of spin-polarized electrons, the use of which allows for the exploration of spin-dependent processes such as electron exchange and the spin-orbit interaction. Because of the greater complexity of inelastic scattering reactions, where radiative decay of the excited atom produces polarized photons, these processes in particular have greatly benefited from the recent experimental developments. As well, improvements in laser technology have allowed for the production of fine- and hyperfine-structure resolved excited atomic states which can be subsequently used for superelastic scattering reactions.

Sodium in particular has been an extremely popular target for electron-atom experiments and calculations. With an atomic number of 11, sodium is a more complex atom than either hydrogen or lithium and at the same time is light enough that relativistic effects are quite small. One indication of this is the fact that its fine-structure levels are nearly degenerate. In addition, sodium is easy to work with experimentally. With the development of superelastic scattering experiments, the fine-structure levels of this atom can be resolved. These superelastic reactions can be described as the time-reverse of inelastic scattering reactions. However, the experiments carried out so far are not strictly the time-reversal of one another since the precision of lasers allows for the production of specific excited *hyperfine* states to be used for superelastic collisions. Inelastic experiments are unable to resolve these states due to the extremely small differences in their energy levels. Zeman *et al.* [1] have investigated the differences between these two approaches and have confirmed that for sodium they are negligible.

The scattering parameters which provide the most sensitive tests of theoretical methods are those which involve the use of spin-polarized electrons. The National Institute of Standards and Technology (NIST) group have performed superelastic e^--Na experiments [2,3] and, with the help of Hertel *et al.* [4], have produced results for the singlet and triplet contributions to $L_\perp$ (the angular momentum transferred perpendicular to the scattering plane) and the ratio r of triplet to singlet cross sections. The superelastic scattering technique has also been used by Nickich *et al.* [5] to measure S_A, the spin asymmetry parameter for the fine-structure resolved $(3\mathrm{p})\,^2\mathrm{P}_{1/2,3/2}$ states. In contrast Hegemann *et al.* [6] have also used spin-polarized electrons, but for an inelastic scattering experiment and at energies slightly lower than are considered here. They measured the parameter T_y (or $T_\perp$) which, in the nonrelativistic limit, is equal to the degree of contraction of the electron spin-polarization perpendicular to the scattering plane. As well, other experiments have been proposed [7,8] which would allow for the measurement of a complete set of parameters yielding enough information

[a] *Current address:* Department of Mathematics, University of Nottingham, Nottingham NG7 2RD, UK

[b] *Current address:* Atomic and Molecular Physics Laboratories, Research School of Physical Sciences and Engineering, Australian National University, 0200 Canberra, Australia

[c] e-mail: `stauffer@yorku.ca`

for a "perfect scattering experiment" (assuming relativistic effects are negligible). For alkalis heavier than sodium there have not been any experiments performed to date which yield differential parameters (other than cross sections) in the intermediate energy range, even for unpolarized incident electrons, although two are currently underway. These are the superelastic measurements of differential Stokes parameters for rubidium [9] and inelastic asymmetry measurements for cesium [10]. A detailed review of the collisional alignment and orientation parameters for unpolarized incident electrons has been given by Andersen *et al.* [11] and for spin-polarized incident electrons by Andersen *et al.* [12], while the generalized STU-parameters are reviewed in Bartschat [13], and Kessler [14].

On the theoretical side the most sophisticated method is the convergent close-coupling (CCC) formalism [15]. This method calculates the total non-relativistic wavefunction of the scattering system to an arbitrary degree of accuracy, as it includes a sufficient number of higher discrete and continuum states for convergence to be achieved. This method was used on sodium by Bray [16]. The second-order distorted-wave Born approximation (DWBA2), developed by Madison *et al.* [17], has also proven to be very accurate. Here the electron-atom interaction is described by a two-step process which allows for more accurate calculations at lower incident electron energies where the approximation of an instantaneous interaction made by first-order methods becomes invalid. The DWBA2 has been used for electron impact excitation of both sodium [18] and potassium [19]. As well, a very accurate coupled-channel optical (CCO) approximation has been employed for sodium [20] and potassium [21]. In the low energy regime, the nonperturbative coupled-channel R-matrix method has been used to calculate a complete set of scattering parameters for the excitation of sodium to a number of different states. The results of these can be found in Trail *et al.* [22] and Zhou *et al.* [23].

All of these methods, however, are non-relativistic and therefore become increasingly inaccurate for heavier atoms. In this work we use the relativistic distorted-wave (RDW) approximation which was first developed by Zuo *et al.* [24] and extended to alkali atoms by Zeman *et al.* [25]. Here, both the atom and the continuum electron are treated in the Dirac formalism. The use of this method with sodium is expected to yield results similar to those from the first-order distorted-wave Born approximation (DWBA) and can thus be used as a verification of the method in the non-relativistic regime. For heavier alkalis the RDW method is used to determine where relativistic effects occur and therefore where the above non-relativistic methods are likely to fail.

In this paper we have used the RDW method for the electron impact excitation of sodium, potassium and rubidium to their first $(n\mathrm{p})\,^2\mathrm{P}_{1/2,3/2}$ levels in the intermediate energy range. Extensive results have already been reported for the excitation of cesium to a number of different states [25–28]. The parameters presented here include differential cross sections, differential and integrated Stokes parameters, generalized STU-parameters and other collisional alignment and orientation parameters which have been previously measured. A brief review of the RDW method and the various scattering parameters is given in Section 2. The various results as well as comparisons with experiments and other theories are found in Section 3. The conclusions are drawn in Section 4.

2 Theory

The RDW method [24] takes relativistic effects into account by treating both the atomic and continuum electron wavefunctions in the Dirac formalism. The atomic orbitals were obtained by using a multi-configuration Dirac-Fock algorithm [29]. Our choice of the distortion potential used to calculate the distorted waves is the well accepted static potential of the final channel. Details of this method, as applied to alkali atoms, are given in Zeman *et al.* [25].

It is important to determine scattering parameters other than the cross section in order to obtain a more detailed understanding of the collision process. Also, it is important to produce scattering parameters as a function of the scattering angle, since the integrated parameters mask effects which occur at larger scattering angles. To obtain the maximum amount of information about the interaction, *i.e.*, to perform a "perfect scattering experiment", parameters which depend on the spin-polarization of the incident electron must also be obtained.

The Stokes parameters are a measure of the polarization of the photon which is emitted during the decay of the atom after electron impact excitation. These give an indication of the magnetic sublevel distribution of the excited atomic state. The three Stokes parameters which are normally measured are

$$P_1 = \eta_3 = \frac{I(0^\circ) - I(90^\circ)}{I(0^\circ) + I(90^\circ)} \tag{1a}$$

$$P_2 = \eta_1 = \frac{I(45^\circ) - I(135^\circ)}{I(45^\circ) + I(135^\circ)} \tag{1b}$$

$$P_3 = -\eta_2 = \frac{I_+ - I_-}{I_+ + I_-} \tag{1c}$$

where $I(\beta)$ is the intensity of emitted photons polarized at an angle β with respect to the direction of the incident electron while $I_\pm$ represents the intensity of left- and right-handed circularly polarized photons. These intensities are measured perpendicular to the scattering plane. The calculation of these parameters can include the depolarization due to averaging over the excited hyperfine states. We adopt the η_i notation if this is the case, and the P_i notation if the hyperfine depolarization coefficients are omitted. For the case where the fine-structure excited states are not resolved the reduced Stokes parameters $\bar{P}_i$ [11] are defined when depolarization due to averaging over the fine-structure states is neglected. Details regarding the calculation of the Stokes parameters are given in Bartschat

et al. [30]. It should be noted that these Stokes parameters are defined for unpolarized incident electrons and therefore mask certain features of the interaction which are dependent upon the electron spin-polarization. For light emitted by an atom after excitation by spin-polarized electrons the *generalized* Stokes parameters [12,31] are used to describe the polarization state of the photon. Unfortunately, there are no experimental or other theoretical data for these parameters for the atoms considered here.

The change in spin-polarization of the continuum electron is described by the generalized STU-parameters. These parameters have been reviewed in detail in Bartschat [13] and Kessler [14]. For an incident electron with spin-polarization $\mathbf{P} = P_x\hat{\mathbf{x}} + P_y\hat{\mathbf{y}} + P_z\hat{\mathbf{z}}$ the spin-polarization of the scattered electron is given by

$$\mathbf{P}'=\frac{(S_{\rm P}+T_yP_y)\hat{\mathbf{y}}+(T_xP_x+U_{xz}P_z)\hat{\mathbf{x}}+(T_zP_z-U_{zx}P_x)\hat{\mathbf{z}}}{1+S_{\rm A}P_y}\,. \tag{2}$$

Here we have assumed the collision frame of reference where $\hat{\mathbf{z}}$ is defined to be the direction of the incident electron and $\hat{\mathbf{y}}$ is perpendicular to the scattering plane. The asymmetry parameter $S_{\rm A}$ is a relatively simple parameter to measure. It is defined as the left-right asymmetry in the differential cross section after scattering a spin-polarized electron beam from an unpolarized atom, *i.e.*,

$$\sigma = \sigma_{\rm un}(1 + S_{\rm A}P_y) \tag{3}$$

where $\sigma_{\rm un}$ is the differential cross section for an unpolarized electron beam. The experimental determination of the asymmetry parameter is performed by simply measuring

$$S_{\rm A}P_y = \frac{\sigma^{\uparrow} - \sigma^{\downarrow}}{\sigma^{\uparrow} + \sigma^{\downarrow}} \tag{4}$$

where $\uparrow$ indicates that the incident electron beam is spin-polarized in the positive y-direction, and $\downarrow$ in the negative.

Generalizing to spin-polarized atoms [32,33], equation (3) becomes

$$\sigma = \sigma_{\rm un}(1 - A^{\rm ex}P_y^{\rm e}P_y^{\rm A} + A^{\rm so}P_y^{\rm e} + A^{\rm int}P_y^{\rm A}) \tag{5}$$

where the superscripts on P_y refer to the incident electron or the atom, and $A^{\rm so}$ is equal to $S_{\rm A}$. The experimental determination of these three asymmetries is found by measuring

$$A^{\rm ex} = \frac{(\sigma^{\downarrow\uparrow} + \sigma^{\uparrow\downarrow}) - (\sigma^{\uparrow\uparrow} + \sigma^{\downarrow\downarrow})}{(\sigma^{\downarrow\uparrow} + \sigma^{\uparrow\downarrow}) + (\sigma^{\uparrow\uparrow} + \sigma^{\downarrow\downarrow})} \tag{6a}$$

$$A^{\rm so} = \frac{(\sigma^{\uparrow\uparrow} + \sigma^{\uparrow\downarrow}) - (\sigma^{\downarrow\uparrow} + \sigma^{\downarrow\downarrow})}{(\sigma^{\uparrow\uparrow} + \sigma^{\uparrow\downarrow}) + (\sigma^{\downarrow\uparrow} + \sigma^{\downarrow\downarrow})} \tag{6b}$$

$$A^{\rm int} = \frac{(\sigma^{\uparrow\downarrow} + \sigma^{\downarrow\downarrow}) - (\sigma^{\uparrow\uparrow} + \sigma^{\downarrow\uparrow})}{(\sigma^{\uparrow\downarrow} + \sigma^{\downarrow\downarrow}) + (\sigma^{\uparrow\uparrow} + \sigma^{\downarrow\uparrow})} \tag{6c}$$

where in this notation the first and second arrows on each cross section refer to the incident electron and atomic spin-polarization, respectively. The theoretical calculation of these parameters is given in Appendix A.

In the non-relativistic fine-structure approximation [34] LS-coupling, rather than jj-coupling, is employed. Here the quantum numbers L and S of the total electron-atom system are assumed to be separately conserved and the fine-structure atomic states are therefore not resolved. In this approximation the first resonant excited state of an alkali atom is referred to as the $(n{\rm p})\,^2{\rm P}$ state. For such an $L = 1$ state (as well as a $J = 1$ state of an atomic system in a relativistic calculation) there are other sets of scattering parameters which have a simple physical interpretation. These collisional alignment and orientation parameters have been described in detail in Andersen *et al.* [11] for unpolarized incident electrons and in Andersen *et al.* [12] for spin-polarized electrons.

Since most of the experimental and other theoretical results for sodium have been presented in the form of these parameters, we too have calculated some of these parameters in order to compare with the other sets of data. One of these is the angular momentum transferred to the atom perpendicular to the scattering plane. This is simply given as

$$L_\perp = -\bar{P}_3. \tag{7}$$

$L_\perp$ can be separated into its singlet ($S = 0$) and triplet ($S = 1$) components, $L_\perp^{\rm s}$ and $L_\perp^{\rm t}$ [4]. Also in the fine-structure approximation, the exchange asymmetry parameter can be written in terms of these angular momentum parameters as

$$A^{\rm ex} = \frac{4L_\perp - 3L_\perp^{\rm t} - L_\perp^{\rm s}}{3\,(L_\perp^{\rm s} - L_\perp^{\rm t})}\,. \tag{8}$$

Experiments performed to measure these parameters have been done for sodium using the superelastic scattering technique by the NIST group [2,3]. The calculation of the perpendicular angular momentum parameters for superelastic scattering have been presented by Zeman *et al.* [1], who also show that for sodium these parameters are almost identical to those found in the inelastic scattering case. The linear Stokes parameters for sodium (see Eqs. (1a,b)) have also been measured for the superelastic case [35,36]. These are often represented by the parameters

$$P_{\rm lin} = \sqrt{P_1^2 + P_2^2} \tag{9a}$$

$$\gamma = \tfrac{1}{2}\arg(P_1 + iP_2). \tag{9b}$$

For an $L = 1$ system these two parameters represent important physical properties of the atomic charge cloud. The linear polarization $P_{\rm lin}$ is equal to the relative difference between the length and width of the atomic charge cloud in the scattering plane, *i.e.*

$$P_{\rm lin} = \frac{|\psi|^2_{\rm max} - |\psi|^2_{\rm min}}{|\psi|^2_{\rm max} + |\psi|^2_{\rm min}} \tag{10}$$

where ψ is the wavefunction of the exited $L = 1$ state. The charge cloud alignment angle γ represents the direction, with respect to the direction of the incident electron, where the maximum charge cloud density in the scattering plane $|\psi|^2_{\max}$ is found. The minimum charge cloud density in the scattering plane $|\psi|^2_{\min}$ is located perpendicular to $|\psi|^2_{\max}$.

3 Results

3.1 Sodium

Other than hydrogen, sodium has been the most frequently studied alkali for electron-atom collisions. The most sophisticated experiments in the intermediate energy range, where differential parameters other than cross sections have been measured, are those by McClelland *et al.* [2], Scholten *et al.* [3], Nickich *et al.* [5], Scholten *et al.* [35] and Sang *et al.* [36]. The most detailed calculations in the intermediate energy range are the CCC [16,20], and DWBA2 [18]. Since sodium is considered to be a light atom where relativistic effects are negligible, we expect our RDW results to be similar to those obtained from the DWBA and therefore present a sample of our results for this atom as a test of our method in the non-relativistic regime. These results can then give an indication of the accuracy of the various parameters predicted for heavier alkalis where experimental results are scarce. Relativistic effects exhibited by the very sensitive S parameters have already been tested indirectly by comparing with other atoms of similar atomic numbers (see, for example Fig. 9 of Zeman *et al.* [37]) and were found to be reasonably accurate.

We compare our RDW results for the differential cross section for excitation to the unresolved $(3p)\,^2P$ state to the experimental data at various incident electron energies in Figure 1 [1]. The experimental errors are about 50% for Jiang *et al.* [40], usually within 20% for Marinkovic *et al.* [38], about 10–25% for McClelland *et al.* [2] and Scholten *et al.* [3], within 20% for Teubner *et al.* [41] and Buckman and Teubner [42], about 20% for Srivastava and Vuskovic [39] and less than 30% for Shuttleworth *et al.* [43]. Lorentz and Miller [44] have not listed their errors. The RDW cross sections lie above the experimental measurements at larger scattering angles, but the shape of the curves are quite accurate. This is an important point since all of the other scattering parameters involve ratios of various scattering amplitudes so that inaccuracies in the magnitudes of the scattering amplitudes tend to cancel out. Since all of the experimental data, with the exception of the measurements of Jiang *et al.* [40], are relative measurements which have later been normalized in a variety of ways, a comparison of the shapes of the curves is more meaningful than the magnitudes. The measurements of Jiang *et al.* [40] are unfortunately limited to a maximum energy of 22.1 eV and, at that energy, a maximum scattering angle of only 10°. As well, the magnitudes of the experimental points themselves are inconsistent. Teubner *et al.* [41] have renormalized the data of Srivastava and Vuskovic [39] and found them to be consistent with theirs. However, the data of the NIST group [2,3] is consistent with the original data of Srivastava and Vuskovic [39].

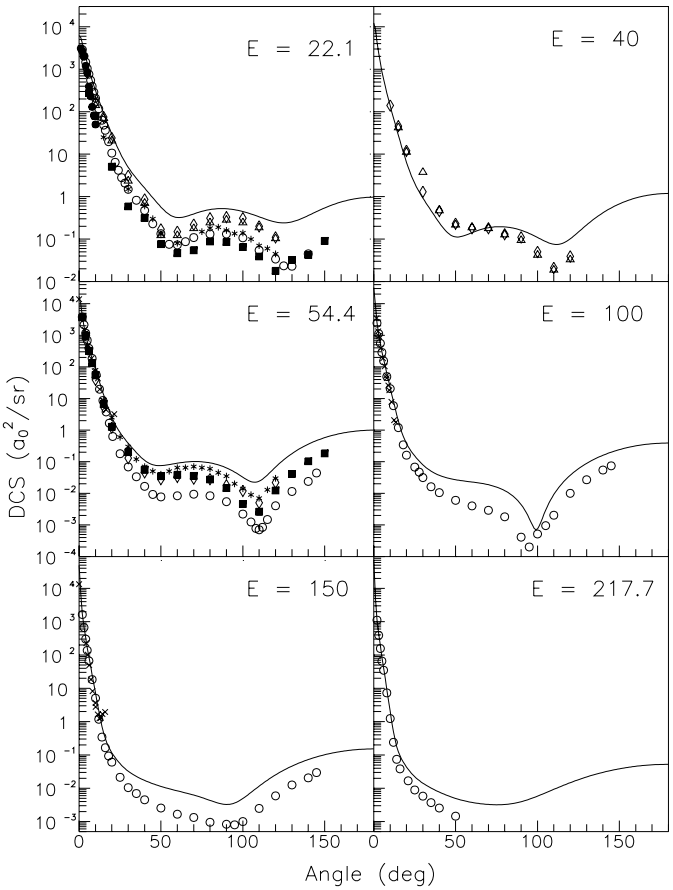

Fig. 1. Comparisons of the differential cross sections with experiment for the excitation of Na to the unresolved $(3p)\,^2P$ state at various energies. ———, RDW; ●, [40]; ■, [38]; Δ, [2,3]; *, [44]; ○, [41], [42]; ◇, [39]; ×, [43]. See text regarding footnote 1.

In Figure 2 we compare our RDW differential cross sections with other theoretical calculations at two different energies. Apart from the most sophisticated calculations previously mentioned [16,18,20] we have also included a first-order DWBA calculation [18] in this figure. Other theoretical methods which have not been represented here, in order to keep some clarity in the figures, are the two-potential localized exchange (TPLE) approximation [45], the CC4 method [46] and another first-order DWBA approximation [47]. The latter method employs an optical potential rather than the usual static potential used by the RDW and DWBA methods. Therefore, in the non-relativistic regime, our results should agree most closely with the DWBA results. This is indeed the case if one

[1] In this and subsequent figures for Na where the incident electron energy is listed as 22.1 eV the data of McClelland *et al.* [2], Marinkovic *et al.* [38] and Srivastava and Vuskovic [39] and the DWBA2 calculations [18] are actually for 20 eV. The curves do not change appreciably for such small energy differences.

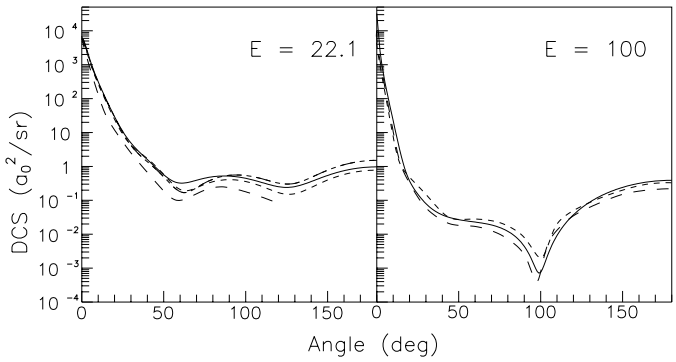

Fig. 2. As in Figure 1 for various theoretical computations. ———, RDW; - - -, DWBA2 [18]; – –, CCC [16] and CCO [20]; – - –, DWBA [18]. See text regarding footnote 1.

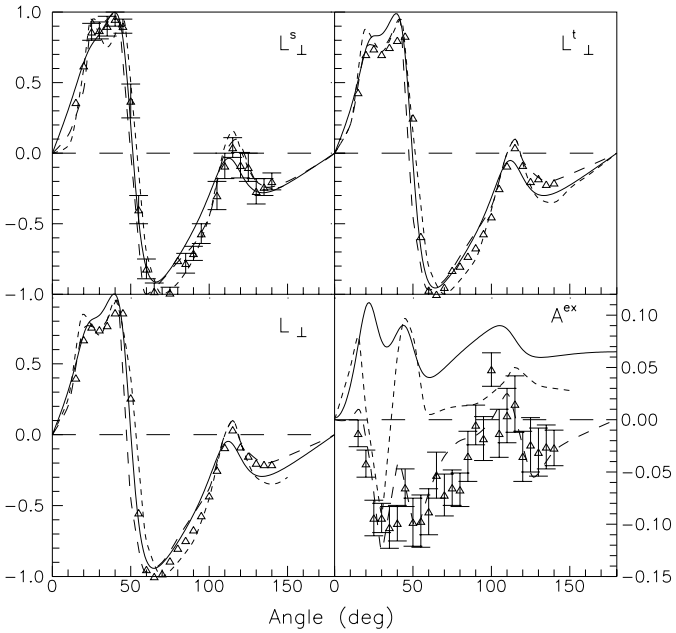

Fig. 3. $L_\perp$, $L^s_\perp$, $L^t_\perp$ and A^{ex} for the excitation of Na to the $(3p)\,^2P$ state at an incident energy of 40 eV. ———, RDW; - - -, DWBA2 [18]; – –, CCC [16]; Δ, [2,3].

examines the data shown at 22.1 eV. As the incident electron energy is increased, the curves tend to converge towards each other (except for the TPLE calculations) thus validating the use of first-order methods (including the RDW) at higher energies. All of the theoretical cross sections tend to be greater than the experimental measurements at larger angles, even though the agreement at smaller angles is very close. This indicates some sort of systematic error which is being made by either all of the calculations or all of the experiments. We have not shown the differential cross sections for the fine-structure resolved $(3p)\,^2P_{1/2,3/2}$ states since their ratio rarely differs from two by more than 5%. This is an indication of the validity of the fine-structure approximation for sodium.

The Stokes parameters are a measure of the polarization of the photon emitted by the excited atom and thus provide information about the excited atomic state. The circular Stokes parameter η_2^y is proportional to the perpendicular angular momentum transferred to the atom, $L_\perp$. In LS-coupling we can separate this parameter into its singlet and triplet components, $L^s_\perp$ and $L^t_\perp$. The NIST group [2,3] have measured these parameters for the case of superelastic scattering from the $(3p)\,^2P_{3/2}(F=3)$ state of sodium. From these measurements one can also obtain the exchange asymmetry parameter A^{ex}, assuming LS-coupling, as shown by (8). We have calculated these parameters and compare them to experiment in Figure 3 at 40 eV. The differences between the inelastic and superelastic scattering parameters for sodium are negligible [1], so they can therefore be used interchangeably. Also shown are various theoretical curves, all of which have been calculated for the corresponding inelastic scattering to the unresolved $(3p)\,^2P$ state. These curves correspond to the CCC formalism [16] as well as the DWBA2 [18]. Other theoretical results which, due to clarity, are not shown in these figures include those obtained from the TPLE approximation [45,48], the DWBA [47] and the CCO [20] and CC4 [46] methods. For the three perpendicular angular momenta all calculations give similar results (except for the TPLE) and are in reasonable agreement with the experimental data. However, it is evident that A^{ex} is a much more sensitive parameter, since from equation (8) it involves the differences of angular momentum parameters which are usually almost equal to each other. Our RDW results for this parameter, along with the DWBA [18], DWBA [47] and CC4 curves [46], are very inaccurate. The DWBA2 method is somewhat better, while the CCO and CCC results are much more accurate and demonstrate the necessity of effectively including all channels, including those representing the continuum, for such a sensitive parameter.

Like the differential Stokes parameters, the generalized STU-parameters provide a deeper insight into the scattering interaction than the differential cross sections do. Whereas the Stokes parameters describe the state of the excited atom, the generalized STU-parameters describe the state of the scattered electron. The most straight forward parameter to measure is the asymmetry parameter S_A. It is simply the difference between spin-up and spin-down cross sections as shown in equation (4). There have been two measurements of this parameter, both using the superelastic scattering mechanism. The experiments by the NIST group [2,3] have yielded $\bar{S}_A$ (here the bar indicates superelastic scattering) results indirectly by measuring circularly polarized photon intensities, while Nickich *et al.* [5] have directly measured $\bar{S}_A$ for both of the $(3p)\,^2P_{1/2,3/2}$ states separately. It can be shown that $\bar{S}_A = S_P$, provided that the frame of reference is the same for the inelastic and superelastic experiments under consideration [34]. If both experiments are performed in their respective collision reference frames then their y-directions are opposite to each other which results in $\bar{S}_A = -S_P$.

In Figure 4 we show the spin polarization S_P for excitation to the $(3p)\,^2P_{1/2}$ state at an incident electron energy of 22.1 eV. As well as the two sets of experimental data, we compare our results with the CCC calculation [16] and the

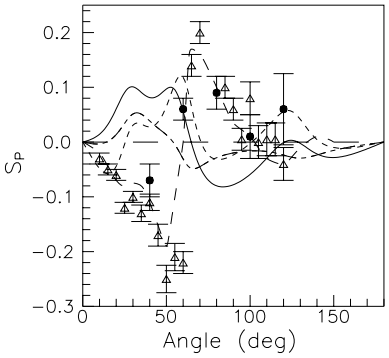

Fig. 4. Spin polarization S_P for the excitation of Na to the $(3p)\,^2P_{1/2}$ state at an incident energy of 22.1 eV. ———, RDW; - - -, DWBA2 [18]; – –, CCC [16]; – - –, DWBA [18]; •, [5]; Δ, [2]. See text regarding footnote 1.

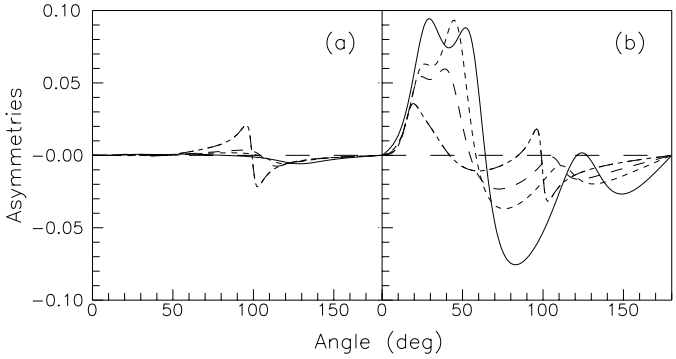

Fig. 5. Asymmetries for Na at incident energies (in eV) of ———, 22.1; - - -, 40; – –, 54.4; – - –, 100. (a) A^{so} for the $(3p)\,^2P$ state. (b) S_A for the $(3p)\,^2P_{1/2}$ state.

DWBA2 and DWBA [18]. Other calculations not shown in this figure include the DWBA [47] and TPLE approximation [49]. The CCC results compare well with both sets of experimental data, which are not themselves always in agreement with each other. The other calculations are insufficient in describing the spin polarization, including even the DWBA2. The difference between the DWBA and DWBA2 curves [18] provides a direct demonstration of the effects of the second-order terms. However here, unlike for the other parameters, our RDW results are not in total agreement with the DWBA curve. As will be shown in Figure 5, the fine-structure approximation is valid for this case so that S_P for the $(3p)\,^2P_{3/2}$ state is approximately a factor of (-0.5) times that for the $(3p)\,^2P_{1/2}$ state, and is therefore not shown.

In Figure 5 we show the RDW results for the S_A and A^{so} parameters for excitation to the $(3p)\,^2P_{1/2}$ and $(3p)\,^2P$ states, respectively, at various energies. A^{so} is simply the average of S_A over the two fine-structure states and represents the strength of the spin-orbit interaction (see Appendix A). S_A is influenced by both the relativistic spin-orbit interaction and the non-relativistic electron exchange. A^{so} is very small for sodium, although it increases slightly at 100 eV. This increase can be attributed to the deeper penetration of the incident electron into the atom. S_A is also quite small in magnitude and is seen to decrease as the energy increases. This decrease occurs because the value of the incident electron energy is moving farther away from the energy of the atomic electrons (especially the valence electron). Since at 100 eV the exchange terms are so small, the fine-structure approximation is in fact invalidated at larger scattering angles even though the spin-orbit interaction is not very strong.

In summary, the comparisons of our RDW results with experiments and other theories for sodium provide a thorough test of the RDW formalism in the non-relativistic regime. These comparisons are very favorable for most of the scattering parameters with the exception of the spin-sensitive asymmetry parameters. However, for these parameters, it has already been shown [18] that a first-order method is insufficient. For heavy atoms, where the relativistic spin-orbit interaction dominates over electron exchange, we have found that indirect comparisons of our S parameters with experiment are favourable. We can therefore conclude that the RDW method is accurate in all cases except those describing the electron exchange mechanism in the spin-sensitive parameters.

3.2 Potassium

Potassium, with an atomic number of 19, has also been generally considered to be an atom light enough that relativistic effects can be neglected. However, there have not been any tests performed of the validity of the fine-structure approximation for this atom (experimental or theoretical). In fact, there have not been any measurements made at all of differential parameters other than cross sections. Since the fine-structure approximation fails for sodium at larger energies, we can expect the same (at least) to occur for potassium.

In Figure 6 the differential cross sections for the unresolved $(4p)\,^2P$ state at various energies are shown. These are compared with the inelastic scattering experiments of Vuskovic and Srivastava [50] with experimental errors listed as 18%, Buckman *et al.* [51] with uncertainties of under 20% and Williams and Trajmar [52] with errors as great as 50%. All three experiments measured relative values which were later normalized in various ways. We also compare our results with the theoretical calculations using the DWBA2 [19], the DWBA [53] and the 17CCO6 approximation [21]. Verma and Srivastava [53] give DWBA results for several different choices of distortion potential. We have plotted their DWBA results for the case where the final distortion potential is used in both the initial and final channels, which is the potential that we have used, and which has been found to best approximate higher order effects [54]. Other theoretical methods which have not been shown in Figure 6 include the unitarized distorted-wave Born approximation (UDWBA) [55] and the 4CCO method [56]. As was the case with sodium, the theoretical results tend to converge to one another as the energy increases. The agreement is excellent with the experimental data at small scattering angles ($< 15°$). At larger angles the general shape of our curves compares well with

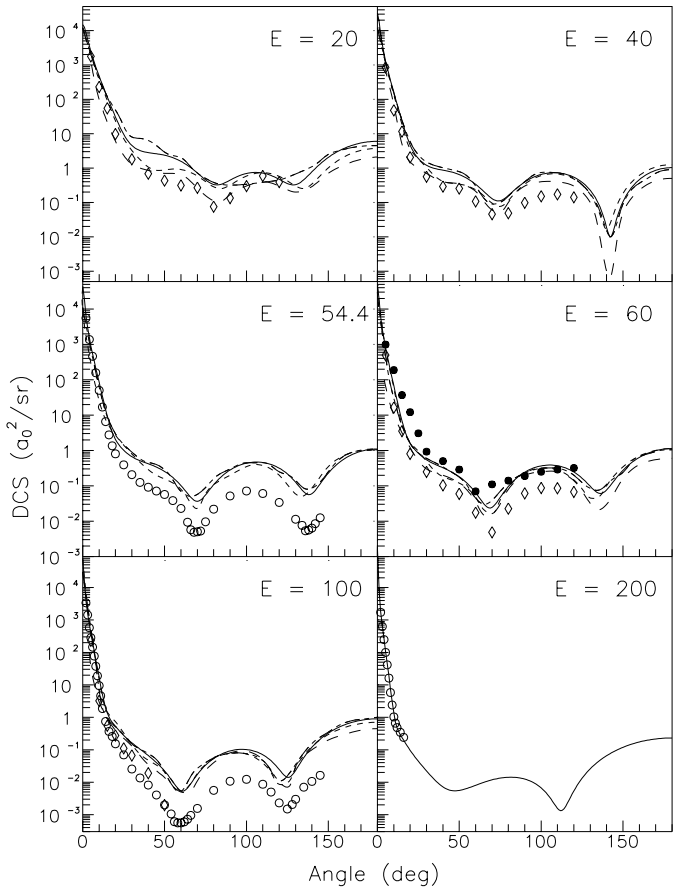

Fig. 6. Differential cross sections for excitation of K to the $(4p)\,^2P$ state at various energies. ———, RDW; - - -, DWBA2 [19]; – –, 17CCO6 [21]; – - –, DWBA [53]; ◇, [50]; ○, [51]; ●, [52].

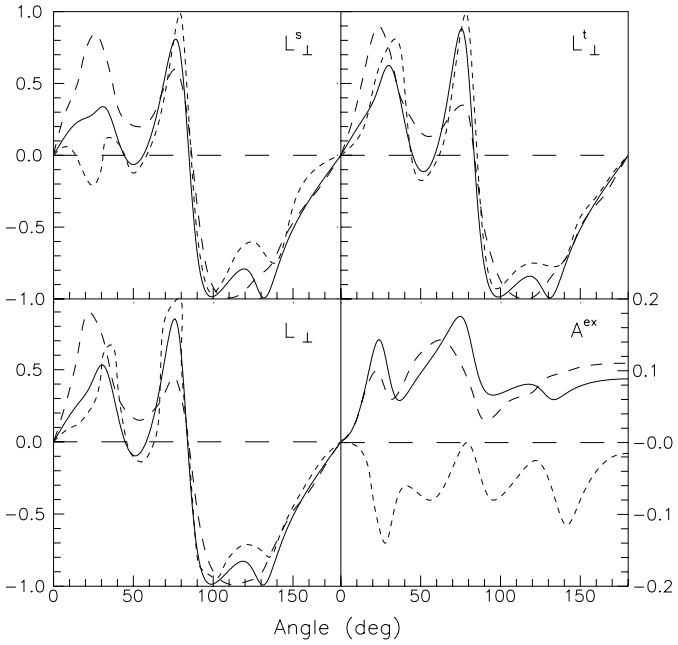

Fig. 7. $L_\perp$, $L^s_\perp$, $L^t_\perp$ and A^{ex} for the excitation of K to the $(4p)\,^2P$ state at an incident energy of 20 eV. ———, RDW; - - -, 17CCO6 [21]; – –, DWBA [53].

the experimental results of Vuskovic and Srivastava [50] and Buckman *et al.* [51], but the magnitudes tend to be larger. As was the case with sodium, all of the theoretical curves are greater in magnitude than the experimental results (with the exception of the one set of data points in Williams and Trajmar [52]). Out of all of the theoretical curves, the 17CCO6 calculations have the smallest cross section magnitudes. This is particularly evident at smaller energies. One particularly encouraging feature of our RDW results at 100 eV is the relative magnitudes of the two minima. The ratio of the two minima is best approximated by the RDW curve. As will be shown later in this section, the non-relativistic fine-structure approximation is invalid at this energy, although the spin-orbit interaction is still relatively weak. Future work needs to be done in this region to determine whether this feature of the differential cross section is a result of relativistic effects. As well, at 200 eV the RDW cross sections are in excellent agreement with experiment, although data only exists up to a maximum scattering angle of 16°. At this angle for other energies, however, our curves are already visibly greater in magnitude than the experimental points. The ratio of the $(4p)\,^2P_{3/2}$ differential cross sections to the $(4p)\,^2P_{1/2}$ is almost always within 5% of the non-relativistic value of two.

For the differential Stokes parameters there have not been any experimental results to date, but the 17CCO6 formalism [21] has been used to calculate the three perpendicular angular momentum parameters as well as A^{ex} at an incident electron energy of 20 eV. As well, the DWBA [53] has been used to calculate these parameters at several different energies. In Figure 7 we present these parameters at 20 eV. The 17CCO6 results are probably more accurate since this method is more sophisticated than the DWBA and, as will be shown later in this section, relativistic effects are not that large for potassium. For the three angular momentum parameters it is encouraging to note that our calculations reproduce the features of the 17CCO6 calculations better than the DWBA. For A^{ex} the RDW and DWBA calculations produce similar results which are in poor agreement with those from the 17CCO6 approximation. As was the case for sodium, the A^{ex} parameter is much more sensitive to higher order effects than the angular momentum parameters. As the energy is increased the exchange asymmetry becomes smaller in magnitude and the values of the three angular momentum parameters approach each other. In Figure 8 we show the $\bar{P}_{lin}$ and γ parameters at energies of 40 and 100 eV. The only other results with which we can compare these parameters to are the DWBA [53] calculations. With the exception of a few discrete angular values, the comparison of these parameters is good. Since for sodium we found the RDW and DWBA methods fairly accurate in predicting these parameters, they are also probably accurate for potassium as well.

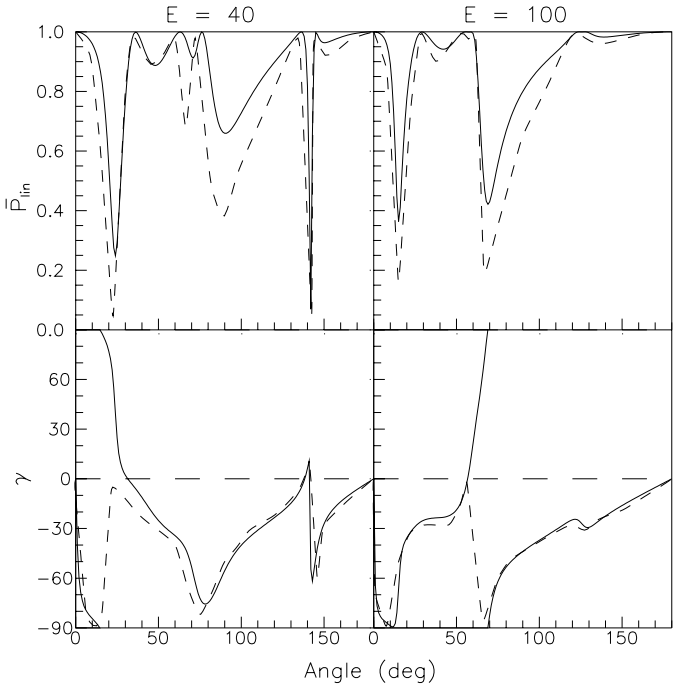

Fig. 8. $\bar{P}_{\rm lin}$ and γ for the excitation of K to the $(4p)\,^2P$ state at incident energies of 40 and 100 eV. ———, RDW; – –, DWBA [53].

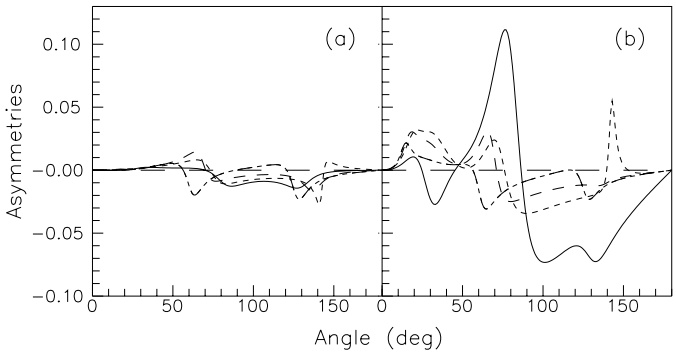

Fig. 9. As in Figure 5 for the excitation of K to the $(4p)\,^2P_{1/2,3/2}$ states at energies of ———, 20; - - -, 40; – –, 60; – - –, 100 eV.

Unlike sodium where the S parameters have been extensively studied, for lower energies at any rate, there have been no experimental or other theoretical studies of the generalized STU-parameters for potassium at any energies. In Figure 9 we show the $S_{\rm A}$ parameter for the $(4p)\,^2P_{1/2}$ state, and the spin-orbit asymmetry $A^{\rm so}$ for the unresolved $(4p)\,^2P$ state, at various energies. Relativistic effects are prominent in areas where $|A^{\rm so}| > 0$, and dominate over electron exchange in areas where $S_{\rm A} \approx A^{\rm so}$. $A^{\rm so}$ for the unresolved state is calculated from the formula

$$A^{\rm so} = \frac{\sigma(1/2)S_{\rm A}(1/2) + \sigma(3/2)S_{\rm A}(3/2)}{\sigma(1/2) + \sigma(3/2)} \qquad (11)$$

and since the ratio of the cross sections for the fine-structure states is close to its non-relativistic value as noted earlier, the $S_{\rm A}$ parameter for the $(4p)\,^2P_{3/2}$ state 4p can be calculated to a good approximation from the data shown in Figure 9 and therefore has not been shown. Here, the spin-orbit interaction is stronger than for sodium. The results at 100 eV in particular fail to follow the non-relativistic approximation. The two dips at this energy show a stronger deviation from the fine-structure approximation, especially the dip at about 125° since the $S_{\rm A}$ parameter is almost equal to $A^{\rm so}$ there, indicating complete dominance of the spin-orbit interaction over electron exchange. However, the spin-orbit interaction is still not that large there, so this dominance is mostly a result of a lack of electron exchange. At any rate, recall that it is the magnitude of this peak that, for the differential cross section, is in correct proportion to the magnitude of the other peak according to experiment.

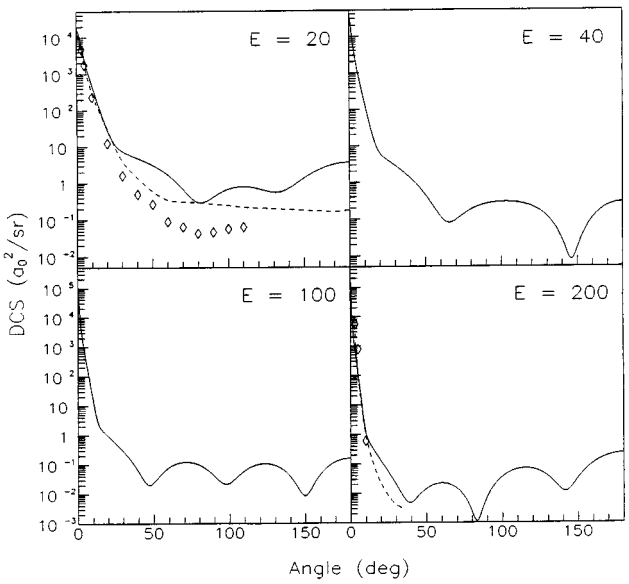

Fig. 10. Differential cross sections for the excitation of Rb to the $(5p)\,^2P$ state at various energies. ———, RDW; – –, DWBA [58]; ⋄, [57].

3.3 Rubidium

Rubidium has been the least studied alkali for electron-atom interactions. On the theoretical front, this may well be because with an atomic number of 37 it is considered heavy enough to probably warrant relativistic treatment, but light enough that theorists have chosen to test their relativistic models on cesium. However, since we have found potassium to exhibit relativistic effects we certainly expect rubidium to do so as well.

The differential cross section calculations for the excitation to the unresolved $(5p)\,^2P$ state are shown in Figure 10 for various energies. They are compared to the experimental data of Vuskovic *et al.* [57] and some DWBA results of Pangantiwar and Srivastava [58]. The distortion potential used for the DWBA results is the initial static potential in the initial channel, and the final static potential in the final channel. We have used the final static

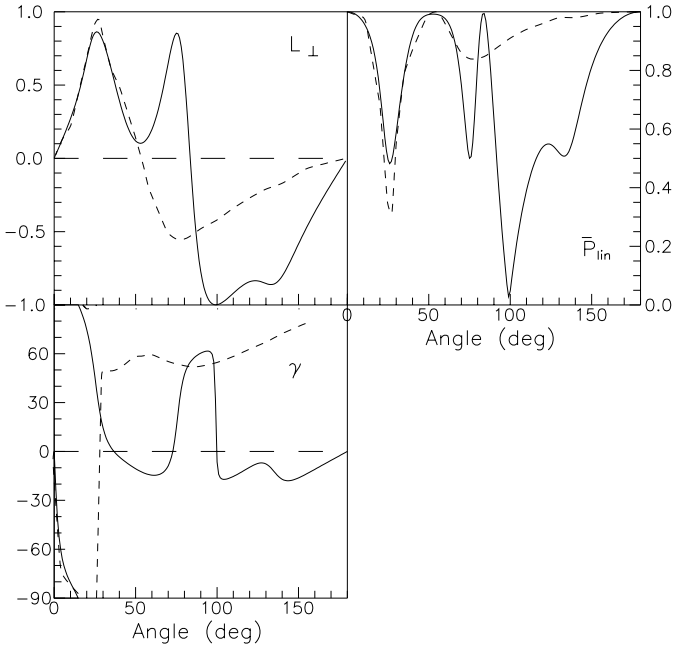

Fig. 11. $L_\perp$, $\bar{P}_{\rm lin}$ and γ for the $(5p)\,^2P$ state of Rb at an incident electron energy of 20 eV. ———, RDW; – –, DWBA [58].

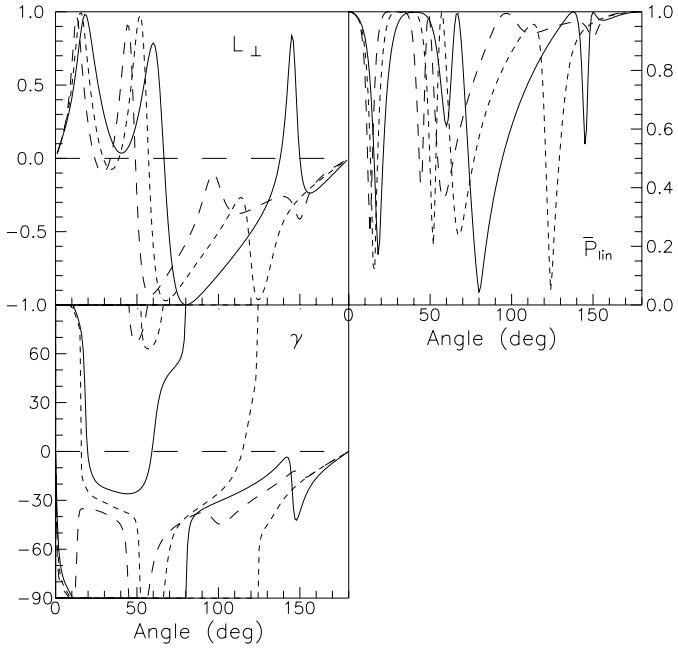

Fig. 12. $L_\perp$, $\bar{P}_{\rm lin}$ and γ for the $(5p)\,^2P$ state of Rb at various energies. ———, 40; - - -, 60; – –, 100 eV.

potential in both channels. However, for the parameters considered in Pangantiwar and Srivastava [58], we have found that our RDW results are only marginally affected by this change in distortion potential. The experimental errors are listed as 20% for scattering angles less than 50° and between 30 and 50% for scattering angles greater than 50°. At small scattering angles our calculations are in excellent agreement with both sets of data at the two available energy values of 20 and 200 eV. At other angles we can only make comparisons at 20 eV. This may be a little low for producing accurate results using the RDW method, but the one minimum exhibited by the experimental data does correspond to a dip in our RDW curve. The DWBA curve, however, appears almost structureless at larger scattering angles. The difference between the RDW and DWBA calculations should only be the inclusion of a relativistic formalism, so if we are to believe the DWBA cross section then relativistic effects are indeed very prominent for rubidium.

There are presently no experimental predictions with which to compare the RDW differential Stokes parameters to, although there is currently a superelastic scattering experiment underway which is expected to yield measurements for these parameters [9]. In Figure 11 we present parameters ($L_\perp$, $\bar{P}_{\rm lin}$ and γ) which completely describe the polarization of the emitted photons after the $(5p)\,^2P$ state has been excited by unpolarized electrons at 20 eV. The RDW results for these are compared to those from the DWBA of Pangantiwar and Srivastava [58]. At smaller scattering angles the comparison is good, but at larger angles the DWBA curves tend to become structureless (as was the case with the differential cross section). These parameters calculated by the RDW method were seen to

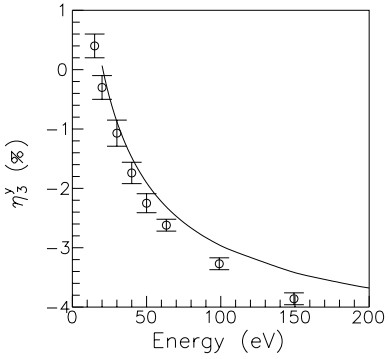

Fig. 13. The integrated Stokes parameter η_3^y for the $(5p)\,^2P_{3/2}$ state of Rb. ———, RDW; ○, [59]

compare quite accurately to experiment for sodium, and should therefore be reliable here as well. The RDW calculations at higher energies are shown in Figure 12.

For the integrated Stokes parameters, the only data with which we can compare our results is for the η_3^y parameter for the $(5p)\,^2P_{3/2}$ state. This parameter is shown in Figure 13 along with the experimental results of Chen and Gallagher [59]. Corrections due to cascade interactions have not been made to these measurements. Nevertheless, the agreement between the RDW calculations and the experimental measurements is quite good especially at lower energies.

In Figure 14 we show the asymmetry parameter $S_{\rm A}$ for excitation to the $(5p)\,^2P_{1/2}$ state and the spin-orbit asymmetry $A^{\rm so}$ for excitation to the unresolved $(5p)\,^2P$ state. The spin-orbit asymmetry shows moderately strong relativistic effects as the $A^{\rm so}$ parameter rises to almost 0.3 at an energy of 60 eV. The $S_{\rm A}$ parameter has the same value in this region, indicating that the asymmetry is due

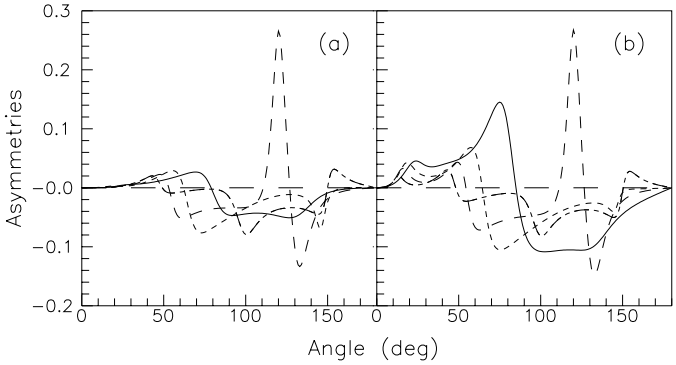

Fig. 14. As in Figure 9 for the excitation of Rb to the $(5p)\,^2P_{1/2,3/2}$ states.

almost entirely to relativistic effects. This peak in particular should be experimentally measurable, even though the peaks for these parameters correspond to minima in the differential cross sections.

4 Conclusions

We have used the RDW method for the electron impact excitation of the first $(np)\,^2P_{1/2,3/2}$ states of sodium, potassium and rubidium in the intermediate energy range. The scattering parameters calculated include the differential cross sections, differential and integrated Stokes parameters and the generalized STU-parameters. As well, we have calculated some collisional alignment and orientation parameters in order to compare with experimental results. For sodium there have been numerous experimental and other theoretical results with which to compare. It is for this reason that we have considered sodium with our RDW formalism. Although sodium is too light to exhibit significant relativistic effects, available data for comparisons for heavy atoms is scarce. The detailed comparisons we were able to make with sodium therefore gives an indication of where our RDW method should yield reliable results for heavier atoms where we often do not have other data with which to compare.

For sodium, we have in fact found that at higher energies (approaching 100 eV) the fine-structure approximation does not to hold, but only because electron exchange becomes very small – the spin-orbit interaction is still quite weak. Our sodium cross sections improve as the incident electron energy increases. The Stokes parameters compare well with experiment, but the spin-sensitive S_P and A^{ex} parameters are found to be inaccurate. However, these inaccuracies are consistent with other first-order calculations, demonstrating the need for more sophisticated calculations for such sensitive parameters.

Potassium has also been a popular target for experimenters and other theorists. As is the case for sodium, calculations other than our RDW approximation have been performed in the fine-structure approximation. Our results show that the spin-orbit interaction is visible at all energies and often dominates over the electron exchange mechanism for the generalized STU-parameters. However, the spin-orbit interaction is still relatively weak. Again our cross sections improve with increasing energy. The differential Stokes parameters compare well with other calculations, but once again A^{ex} is different from that calculated in the more accurate 17CCO6 approximation, but compares well with the DWBA calculation (as it should).

The results for rubidium show definite relativistic effects indicating a necessity for using relativistic methods. Unfortunately, there is a lack of data with which to compare much of these data. At 200 eV the differential cross sections compare well with experiment in the small angular region where data is available. From our sodium (and potassium) comparisons we expect that the scattering parameters dealing with unpolarized incident electrons are accurate. Although the asymmetry parameters have been found to be inaccurate in the non-relativistic region where electron exchange dominates, comparisons of the S parameters produced by the spin-orbit interaction for heavy atoms (see, for example [37]) imply that these parameters should be accurate in regions where the spin-orbit interaction is dominant. We are therefore confident in our predictions of the relativistic effects exhibited by the parameters in Figure 14 for rubidium.

We would like to thank Prof. D. H. Madison for performing some DWBA calculations for us. We are grateful to Dr. I. Bray for sending us detailed results of his calculations. This work was supported in part by the Natural Sciences and Engineering Research Council of Canada.

Appendix A: Calculation of Asymmetry Parameters

If electrons with spin polarization P^e perpendicular to the scattering plane interact with atoms with spin polarization P^A, also perpendicular to the scattering plane, then the differential cross section can be written as [32,33]

$$\sigma = \sigma_{un}(1 - A^{ex}P^eP^A + A^{so}P^e + A^{int}P^A) \qquad \text{(A1)}$$

where σ_{un} is the differential cross section for unpolarized electrons scattering from unpolarized atoms. For excited states where the fine-structure levels are unresolved A^{ex} corresponds to the asymmetry caused by electron exchange alone while A^{so} corresponds to the asymmetry caused by the spin-orbit interaction alone. Both processes together produce an interference asymmetry A^{int}. If the fine-structure states are resolved then the causes of these asymmetries can no longer be separated into these three categories. For example, electron exchange then contributes to A^{so}, and this parameter is therefore normally referred to as simply the asymmetry parameter S_A.

In this appendix we derive expressions for these three asymmetries in analogy to the derivation of S_A given in Bartschat [13]. Starting with the initial electron and atomic density matrices in the collision frame,

$$(\rho^e)^{in} = \tfrac{1}{2}\begin{pmatrix} 1 & -iP^e \\ iP^e & 1 \end{pmatrix} (\rho^A)^{in} = \tfrac{1}{2}\begin{pmatrix} 1 & -iP^A \\ iP^A & 1 \end{pmatrix} \qquad \text{(A2)}$$

we calculate the differential cross section as

$$\sigma = \mathrm{Tr}(\rho)^{\mathrm{out}} = \sum_{M_0 M_0' m_0 m_0'} \{M_0' m_0'; M_0 m_0\} \, (\rho^{\mathrm{e}}_{m_0' m_0})^{\mathrm{in}} (\rho^{\mathrm{A}}_{M_0' M_0})^{\mathrm{in}}. \tag{A3}$$

We have used the definition of the final density matrix [60],

$$\rho^{\mathrm{out}} = T \rho^{\mathrm{in}} T^{\dagger} \tag{A4}$$

where T is the transition operator, and we have defined the quantity

$$\{M_0' m_0'; M_0 m_0\} \equiv \sum_{M_1 m_1} f(J_1 M_1 m_1; J_0 M_0' m_0') \, f^*(J_1 M_1 m_1; J_0 M_0 m_0) \tag{A5}$$

where f represents the scattering amplitudes (which are proportional to the T-matrix elements). J and M refer to total atomic angular momentum quantum numbers, while m is the z-component of the continuum electron. Here we use the notation where the subscripts 0 and 1 refer to initial and final states, respectively. From the hermiticity of the reduced density matrix and the reflection invariance of the scattering amplitudes with respect to the scattering plane,

$$f(J_1 M_1 m_1; J_0 M_0 m_0) = \Pi_1 \Pi_0 (-1)^{J_1 - M_1 + 1/2 - m_1 + J_0 - M_0 + 1/2 - m_0} \times f(J_1 - M_1 - m_1; J_0 - M_0 - m_0) \tag{A6}$$

where Π_0 and Π_1 correspond to the parities of the atomic states, the quantity defined in (A5) has the following properties:

$$\{M_0' m_0'; M_0 m_0\} = \{M_0 m_0; M_0' m_0'\}^* \tag{A7}$$

$$\{M_0' m_0'; M_0 m_0\} = (-1)^{M_0' - M_0 + m_0' - m_0} \times \{-M_0' - m_0'; -M_0 - m_0\}. \tag{A8}$$

Using these properties along with (A1)–(A3) we obtain

$$A^{\mathrm{ex}} = \frac{1}{2\sigma_{\mathrm{un}}} \mathrm{Re} \left[\left\{ \tfrac{1}{2}\tfrac{1}{2}; -\tfrac{1}{2} -\tfrac{1}{2} \right\} - \left\{ \tfrac{1}{2} -\tfrac{1}{2}; -\tfrac{1}{2}\tfrac{1}{2} \right\} \right] \tag{A9}$$

$$A^{\mathrm{so}} = \frac{1}{\sigma_{\mathrm{un}}} \mathrm{Im} \left\{ \tfrac{1}{2}\tfrac{1}{2}; \tfrac{1}{2} -\tfrac{1}{2} \right\} \tag{A10}$$

$$A^{\mathrm{int}} = \frac{1}{\sigma_{\mathrm{un}}} \mathrm{Im} \left\{ \tfrac{1}{2}\tfrac{1}{2}; -\tfrac{1}{2}\tfrac{1}{2} \right\}. \tag{A11l}$$

Note that equation (A10) is equivalent to the definition of S_{A} in Bartschat [13].

References

1. V. Zeman, R.P. McEachran, A.D. Stauffer, J. Phys. B **30**, 3475 (1997).
2. J.J. McClelland, M.H. Kelley, R.J. Celotta, Phys. Rev. A **40**, 2321 (1989).
3. R.E. Scholten, S.R. Lorentz, J.J. McClelland, M.H. Kelley, R.J. Celotta, J. Phys. B **24**, L653 (1991).
4. I.V. Hertel, M.H. Kelley, J.J. McClelland, Z. Phys. D **6**, 163 (1987).
5. V. Nickich, T. Hegemann, M. Bartsch, G.F. Hanne, Z. Phys. D **16**, 261 (1990).
6. T. Hegemann, M. Oberste-Vorth, R. Vogts, G.F. Hanne, Phys. Rev. Lett. **66**, 2968 (1991).
7. N. Andersen, K. Bartschat, Comments At. Mol. Phys. **29**, 157 (1993).
8. N. Andersen, K. Bartschat, Phys. Rev. A **49**, 4232 (1994).
9. Hall B.V., Shen Y., MacGillivray W.R., Standage M.C. Proc. XX Int. Conf. on the Physics of Electronic and Atomic Collisions Abstracts, edited by F. Aumayr, G. Betz and HP. Winter, TH023 (Vienna, 1997).
10. Baum G., oral communication, IX Int. Symp. on Polarization and Correlation in Electronic and Atomic Collisions, (Frascati, 1997).
11. N. Andersen, J.W. Gallagher, I.V. Hertel, Phys. Rep. **165**, 1 (1988).
12. N. Andersen, K. Bartschat, J.T. Broad, I.V. Hertel, Phys. Rep. **279**, 251 (1997).
13. K. Bartschat, Phys. Rep. **180**, 1 (1989).
14. J. Kessler, Adv. At. Mol. Opt. Phys. **27**, 81 (1991).
15. I. Bray, A.T. Stelbovics, Phys. Rev. A **46**, 6996 (1992).
16. I. Bray, Phys. Rev. A **49**, 1066 (1994).
17. D.H. Madison, I. Bray, I.E. McCarthy, J. Phys. B **24**, 3861 (1991).
18. D.H. Madison, K. Bartschat, R.P. McEachran, J. Phys. B **25**, 5199 (1992).
19. D.H. Madison, M. Lehmann, R.P. McEachran, K. Bartschat, J. Phys. B **28**, 105 (1995).
20. I. Bray, I.R. McCarthy, Phys. Rev. A **47**, 317 (1993).
21. I. Bray, D.V. Fursa, I.E. McCarthy, Phys. Rev. A **47**, 3951 (1993).
22. W.K. Trail, M.A. Morrison, Zhou Hsiao-Ling, B.L. Whitten, K. Bartschat, K.B. MacAdam, T.L. Goforth, D.W. Norcross, Phys. Rev. A **49**, 3620 (1994).
23. Zhou Hsiao-Ling, B.L. Whitten, W.K. Trail, M.A. Morrison, K.B. MacAdam, K. Bartschat, D.W. Norcross, Phys. Rev. A **52**, 1152 (1995).
24. T. Zuo, R.P. McEachran, A.D. Stauffer, J. Phys. B **24**, 2853 (1991).
25. V. Zeman, R.P. McEachran, A.D. Stauffer, J. Phys. B **27**, 3175 (1994), corrected in J. Phys. B **28**, 2781.
26. V. Zeman, R.P. McEachran, A.D. Stauffer, Z. Phys. D **30**, 145 (1994), corrected in Z. Phys. D **34**, 293.
27. V. Zeman, R.P. McEachran, A.D. Stauffer, J. Phys. B **28**, 1835 (1995).
28. V. Zeman, R.P. McEachran, A.D. Stauffer, J. Phys. B **28**, 3063 (1995).
29. I.P. Grant, B.J. McKenzie, P.H. Norrington, D.F. Mayers, N.C. Pyper, Comput. Phys. Commun. **21**, 207 (1980).
30. K. Bartschat, K. Blum, G.F. Hanne, J. Kessler, J. Phys. B **14**, 3761 (1981).
31. N. Andersen, K. Bartschat, J. Phys. B **27**, 3189 (1994).
32. P.G. Burke, J.F.B. Mitchell, J. Phys. B **7**, 214 (1974).

33. B. Leuer, G. Baum, L. Grau, R. Niemeyer, W. Raith, M. Tondera, Z. Phys. D **33**, 39 (1995).
34. G.F. Hanne, Phys. Rep. **95**, 95 (1983).
35. R.E. Scholten, G.F. Shen, P.J.O. Teubner, J. Phys. B **26**, 987 (1993).
36. R.T. Sang, P.M. Farrell, D.H. Madison, W.R. MacGillivray, M.C. Standage, J. Phys. B **27**, 1187 (1994).
37. V. Zeman, R.P. McEachran, A.D. Stauffer, Can. J. Phys. **74**, 889 (1996).
38. B. Marinkovic, V. Pejcev, D. Filipovic, I. Cadez, L. Vuskovic, J. Phys. B **25**, 5179 (1992).
39. S.K. Srivastava, L. Vuskovic, J. Phys. B **13**, 2633 (1980).
40. T.Y. Jiang, Z. Shi, C.H. Ying, L. Vuskovic, B. Bederson, Phys. Rev. A **51**, 3773 (1995).
41. P.J.O. Teubner, J.L. Riley, M.J. Brunger, S.J. Buckman, J. Phys. B **19**, 3313 (1986).
42. S.J. Buckman, P.J.O. Teubner, J. Phys. B **12**, 1741 (1979).
43. T. Shuttleworth, W.R. Newell, A.C.H. Smith, J. Phys. B **10**, 1641 (1977).
44. S.R. Lorentz, T.M. Miller, Proc. 16th Int. Conf. on the Physics of Electronic and Atomic Collisions, edited by A. Dalgarno *et al.*, (Amsterdam North-Holland, 1989) p. 198.
45. S.P. Purohit, K.K. Mathur, J. Phys. B **23**, L473 (1990).
46. J. Mitroy, I.I. McCarthy, A.T. Stelbovics, J. Phys. B **20**, 4827 (1987).
47. V.V. Balashov, A.N. Grum-Grzhimailo, Z. Phys. D **23**, 127 (1992).
48. K.C. Mathur, S.P. Purohit, J. Phys. B **22**, L223 (1989).
49. S.P. Purohit, K.C. Mathur, J. Phys. B **26**, 2443 (1993).
50. L. Vuskovic, S.K. Srivastava, J. Phys. B **13**, 4849 (1980).
51. S.J. Buckman, C.J. Noble, P.J.O. Teubner, J. Phys. B **12**, 3077 (1979).
52. W. Williams, S. Trajmar, J. Phys. B **10**, 1955 (1977).
53. S. Verma, R. Srivastava, J. Phys. B **28**, 4823 (1995).
54. D.H. Madison, Comments At. Mol. Phys. **26**, 59 (1991).
55. J. Mitroy, J. Phys. B **26**, 2201 (1993).
56. I.E. McCarthy, J.D. Mitroy, A.T. Stelbovics, J. Phys. B **18**, 2509 (1985).
57. L. Vuskovic, L. Maleki, S. Trajmar, J. Phys. B **17**, 2519 (1984).
58. A.W. Pangantiwar, R. Srivastava, J. Phys. B **21**, 4007 (1988).
59. S.T. Chen, A.C. Gallagher, Phys. Rev. A **17**, 551 (1978).
60. K. Blum, *Density Matrix Theory and Applications* (New York, Plenum, 1981).